Available online at www.sciencedirect.com
SCIENCE DIRECT®
Journal of Power Sources 148 (2005) 55–65
JOURNAL OF POWER SOURCES
www.elsevier.com/locate/jpowsour

Review

The conductivity and characterization of the plasticized polymer electrolyte based on the P(AN-co-GMA-IDA) copolymer with chelating group

Yu-Hao Liang [a], Cheng-Chien Wang [b], Chuh-Yung Chen [a,*]

[a] *Department of Chemical Engineering, National Cheng-Kung University, Tainan 70148, Taiwan*
[b] *Department of Chemical Engineering, Southern Taiwan University of Technology, Tainan 710, Taiwan*

Received 26 January 2005; received in revised form 26 April 2005; accepted 27 April 2005
Available online 23 June 2005

Abstract

The effects of gel polymer with chelating groups on polymer matrix were been characterized by differential scanning calorimeter (DSC) and Fourier transform infrared spectroscopy (FT-IR). The mechanical properties were elucidated using an Instron instrument. The gel polymer, poly(AN-co-GMA-IDA), was made by the copolymerizing acrylonitrile (AN) and (2-methylacrylic acid 3-(bis-carboxymethylamino-2-hydroxy-propyl ester) (GMA-IDA), mixing the product with a plasticizer—propylene carbonate (PC). In a study on gel-type polymer electrolytes, lithium perchloride was doped into the gel polymer. FT-IR and ^{7}Li solid-state NMR spectra elucidate the interactions between lithium ions and the unpaired electrons on the groups based on the gel polymer. Additionally, the ^{7}Li solid-state NMR reveals that lithium ions are preferentially coordinated with the GMA-IDA segments. The glassy transition temperature (T_g) of the gel-type polymer electrolyte increases with the doping of $LiClO_4$, indicating interactions among lithium ions, the plasticizer (PC) and the copolymer. The Arrhenius-like behavior of the conductivity reveals that the charge carries move in a liquid-like environment. The maximum conductivity in this investigation is 2.17×10^{-3} S cm^{-1}. The GMA-IDA unit in the gel-type polymer electrolytes improves the dissociation of the lithium salt and the mechanical strength and conductivity of the electrolytes.

Keywords: Gel-type polymer electrolytes; Chelating polymer; Conductivity; ^{7}Li solid-state NMR; FT–IR

Contents

1. Introduction 56
2. Experimental section 56
   2.1. Materials and experimental procedure 56
   2.2. DSC thermograms 57
   2.3. Solid-state NMR measurements 57
   2.4. Infrared spectroscopy 57
   2.5. Conductivity measurements 57
   2.6. Mechanical properties 57
3. Results and discussion 57
   3.1. Characteristic of copolymer 57
   3.2. Environment of lithium ion doped in gel-type polymer electrolytes 58

* Corresponding author. Tel.: +886 6 2757575 62643; fax: +886 6 2360464.
E-mail address: ccy7@ccmail.ncku.edu.tw (C.-Y. Chen).

0378-7753/$ – see front matter © 2005 Elsevier B.V. All rights reserved.
doi:10.1016/j.jpowsour.2005.04.034

3.3. Thermal characteristics 62
3.4. Ionic conductivity 63
4. Conclusion 64
Acknowledgements 65
References 65

1. Introduction

Since the discovery of ionic conduction in complexes of poly(ethylene oxide) (PEO), solid polymer electrolytes (SPEs) have been extensively investigated [1–3]. The complexes can be used as solid electrolytes in solid-state batteries, electrochromic devices, chemical sensors and other devices. Practical applications depend on polymer electrolyte with conductivity over 1×10^{-3} S cm^{-1}. Unfortunately, the conductivity of most SPEs does not reach this value unless they are in a suitable solvent. Polymer–solvent–salt based electrolytes have been found to have the highest conductivity of current SPEs. These electrolytes, called gel-type polymer electrolytes (GPEs), are fabricated by immobilizing lithium salts and non-aqueous solvents in a polymer matrix. They have so far attracted much attention because of their high ionic conductivity, comparable to that of liquid electrolytes. This high conductivity is resulted from the channel for ion transport in the liquid phases in gel systems [4,11].

Furthermore, the composition of a gel-type electrolyte which determines the ionic conductivity, the electrochemical stability, the compatibility of the gel with the electrodes, and the choice of polymer host is important as well. The effects of the polymer matrix are also reflected in determining the retention of the electrolyte, the mechanical strength and the homogeneity of the system. Moreover, apart from PEO, poly(acrylonitrile) (PAN) [5,6], poly(vinylidene fluoride) (PVdF) [7,8] and poly(methyl methacrylate) (PMMA) [9,10] have also been used as host matrices for gel-type polymer electrolytes. Of these gel-type polymer electrolytes, the PAN-based system has been investigated extensively because of its high ion conductivity at room-temperature and dimensional stability. The elevated conductivity is undoubtedly a favorable character on PAN matrix. Watanabe et al. [11] prepared hybrid-film polymer electrolytes, containing a plasticizer and $LiClO_4$ in a PAN host. The conductivity was found to be related to the molar ratio, [plasticizer]/[$LiClO_4$], but the strength of the mechanical properties decreases against the increasing plasticizer content.

The transport efficiency of lithium ions as well as the general performance of the material often depend on the interactions among the various components of the electrolyte, which, in the case of multi-component system like a gel, might be rather complex. Relevant interactions include, for instance, those within the solvent–salt subsystem, which are responsible for the state of ionic species, as well as those involving the host polymer. The various intermolecular interactions can be elucidated by spectroscopic analysis [12–21].

In this study, a monomer (3-(bis-carboxymethylamino-2-hydroxy*y*-propyl ester) (GMA-IDA) with a strong chelating group, iminodiacetic acid [22–26], is introduced into the PAN matrix by copolymerization to promote the dissociation of the lithium salt and to increase both the free ion content and the dielectric constant. The mechanical properties of the gel-type polymer electrolyte are also improved. Solid-state ^{7}Li NMR, differential scanning calorimeter (DSC), and Fourier transform infrared spectroscopy (FT-IR) were employed to investigate the interaction of lithium ions with both the plasticizer and the polar suspending unit of the copolymer doped with $LiClO_4$.

2. Experimental section

2.1. Materials and experimental procedure

Glycidyl methacrylate (GMA) (Aldrich) was distillated from CaH_2 under reduced pressure and stored under refrigerator at −20 °C. Reagent-grade iminodiacetic acid (IDA) (Avocado) and lithium hydroxide (LiOH) (Rdh) were used without further purification. 2-Methylacrylic acid 3-(bis-carboxymethylamino)-2-hydroxyl-propyl ester) (GMA-IDA) was prepared according to our previous study [22–26]. Poly(AN-co-GMA-IDA) was synthesized by free radical polymerization. Copolymerization of GMA-IDA and acrylonitrile (AN) (Aldrich) was conducted at 60 °C using ammonium peroxodisulfate (APS) (Showa) as initiator and deionized water as medium in a 500 ml four-necked round-bottom flask equipped with an anchor propeller stirrer under nitrogen atmosphere. After 24 h, the flask was cooled down to ambient temperature. The polymer was purified by precipitating reaction mixture into ethanol, and then filtrated. Two precipitation cycles were performed and finally dried under vacuum. Copolymers with 2, 6 and 10% molar ratio of GMA-IDA are denoted as AG2, AG6 and AG10.

Lithium perchlorate ($LiClO_4$) (Fluka) was dried in vacuum prior to use. *N*,*N*-dimethylformanide (DMF) and propylene carbonate (PC) were distilled twice and stored over molecular sieves (4 Å). The hybrid films were obtained by dissolving the copolymer, $LiClO_4$ and PC in DMF at 100 °C and casting the solution onto a polytetrafluoroethylene (PTFE) substrate, and finally stored in a vacuum at 80 °C to remove the solvent. FT-IR preliminary results

confirm the hybrid film no characteristic signals of DMF appeared in.

2.2. DSC thermograms

Thermal analysis of the gel-type polymer electrolytes was carried out in a Dupont DSC 2910 differential scanning calorimeter with a heating at rate 20 °C min^{-1} from −150 to 150 °C.

2.3. Solid-state NMR measurements

^{7}Li MAS with power decoupling NMR were recorded with a Bruker AVANCE-400 NMR spectrometer equipped with a 7 mm double-resonance probe operating at 400.13 MHz for ^{1}H and 155.5 MHz for ^{7}Li. Typical NMR experimental condition were as follows: $\pi/2$ pulse length, 4 μs; recycle delay, 30–150 μs; ^{1}H decoupling power, 65 kHz; spinning speed, 3 kHz. Chemical shifts were externally referenced to the solution LiCl at 0.0 ppm.

2.4. Infrared spectroscopy

FT-IR spectra were recorded at room temperature using a Bio-Rad FT-IR system coupled with a computer. The resolution and scan numbers of IR measurement were 2 cm^{-1} and 64 times, respectively. The spectra were collected in the range between 700 and 4000 cm^{-1}.

2.5. Conductivity measurements

The ionic conductivity of the gel-type polymer electrolytes was obtained using an electrochemical cell consisting of the electrolytic film sandwiched between two stainless steel electrodes. The cell was placed inside a thermostat under Agron condition. Impedance analysis was recorded from 30 to 90 °C, using all Autolab PGSTAT 30 equipment (Eco Chemie B.V., Netherlands) with the software of frequency response analysis (FRA) under an oscillation potential of 10 mV from 100 kHz to 1 Hz in thermostated.

2.6. Mechanical properties

The measurement was conducted via Tensile Test Instrument (Instron 1011) having a test rate at 6 mm min^{-1}.

3. Results and discussion

3.1. Characteristic of copolymer

Copolymers of various compositions were synthesized by the free radical copolymerization of AN and GMA-IDA, according to the procedures [25,26]. Fig. 1 shows the FT-IR spectra of the polymers PAN, AG2, AG6 and AG10. The spectra have characteristic signals at 2900, 1730 and

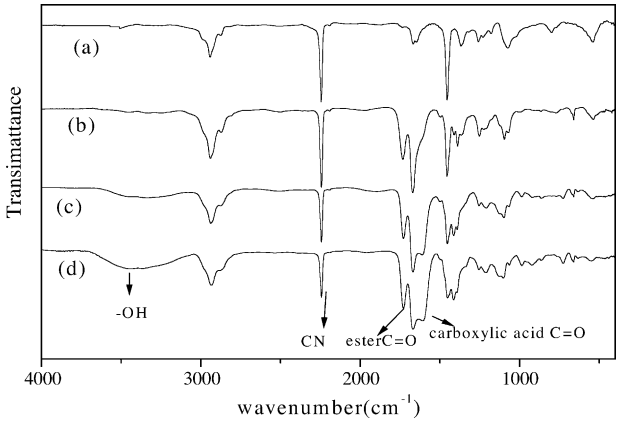

Fig. 1. FT-IR spectra of composite copolymers: (a) PAN, (b) AG2, (c) AG6 and (d) AG10.

Table 1
Chemical compositions of copolymer from elemental analysis

Symbol of polymer	Elemental analysis (C:N:H)	Molar ratio of copolymer (AN:GMA-IDA)
AG2	65.58:24.26:5.91	1:1.94E−2
AG6	63.24:21.70:5.88	1:5.25E−2
AG10	60.16:18.64:5.82	1:10.36E−2

2240 cm^{-1} for the common groups of –CH_3, carbonyl ester (C=O) and C≡N, respectively, in the copolymers. Furthermore, the absorbance peaks at 3430 and 1670 cm^{-1} are referred to as –OH and –COO^- groups, and the intensity of –OH and –COO^- stretching peaks increases with the GMA-IDA content. Table 1 tabulated the results of the elemental analysis on the copolymers. The FT-IR spectra and elemental analyses reveal that the copolymer, poly(AN-co-GMA-IDA), was successfully synthesized and accurately identified.

Fig. 2 presents the FT-IR spectra of C=O stretching in the absorbance range of the –COO^- group for the copolymer (AG2), the plasticizer (PC) and the gel-type polymer (AG2 + PC). The frequency of the absorbance peak of the

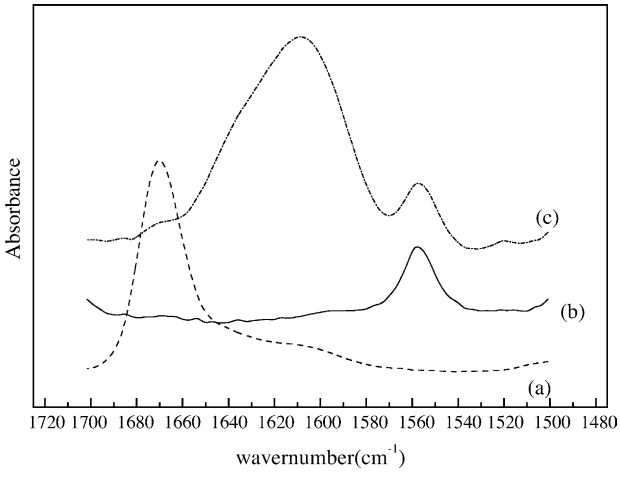

Fig. 2. FT-IR spectra in the C=O stretching region of –COO^- group in AG2: (a) AG2, (b) PC and (c) AG2 + PC.

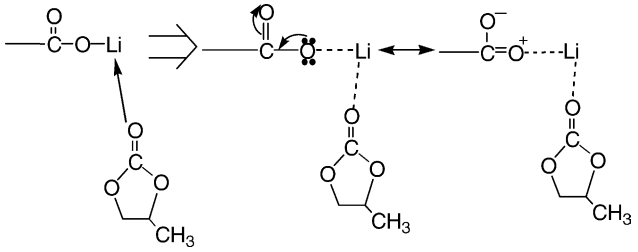

Scheme 1. Schematic representation of interaction between $–COO^-Li^+$ group and PC.

$–COO^-$ shifts downward when the copolymer is mixed with PC to form a gel-type polymer. This shift is attributable to the interactions of PC with the lithium ion of $–COO^-Li^+$, as described in Scheme 1. The lithium ion of the $–COO^-Li^+$ group interacts with the carbonyl group of the PC, when the copolymer is mixed with the PC plasticizer. This effect causes the C=O band to tend to a single bond, reducing the frequency of C=O absorption. Consequently, the movement of the lithium ion of the $–COO^-Li^+$ group increases, improving conductivity.

Table 2 lists the glass transition temperatures for all gel-type polymers investigated in this study. Owing to the PC plasticizer existence, an obviously glass transition temperature is observed at lower temperature in the DSC thermogram of gel-type polymer. However, T_g of the gel-type polymer (without salt) rises with the GMA-IDA content, as shown in Table 2. T_g increases because the molecular movements of the PC solvent is restricted and trapped within cages formed by the polar group in the GMA-IDA unit.

The mechanical properties of gel-type polymers (copolymer/PC = 50/50 wt.%), including Young's modulus and toughness, were examined using an Instron instrument and shown in Figs. 3 and 4 and Table 3. Figs. 3 and 4 show that the mechanical properties of the gel-based copolymers

Table 2
The T_g for all compositions of gel-type polymers

Composition	T_g (°C)			
	PAN	AG2	AG6	AG10
Polymer/PC = 50/50 wt.%	−99	−87	−83	−64
Polymer/PC = 40/60 wt.%	−103	−98	−84	−77
Polymer/PC = 30/70 wt.%	−106	−101	−91	−87
Polymer/PC = 20/80 wt.%	−108	−105	−98	−98

The composition without $LiClO_4$.

Table 3
The mechanical properties of gel-type polymer (polymer 50 wt.%/PC 50 wt.%) from stress–strain test

Mechanical properties	Polymer			
	PAN	AG2	AG6	AG10
Young's modulus (MPa)	17.91	18.40	42.31	63.53
Toughness (MPa)	112	509	1150	1190

The composition without $LiClO_4$.

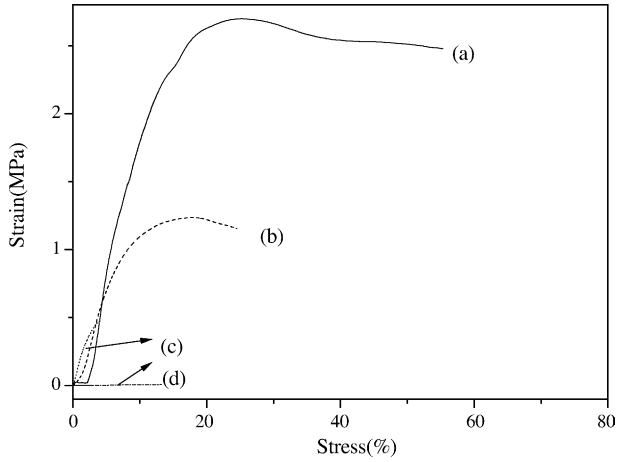

Fig. 3. Stress–strain test for PAN with various PC content: (a) PAN/PC = 50/50 wt.%, (b) PAN/PC = 40/60 wt.%, (c) PAN/PC = 30/70 wt.%, and (d) PAN/PC = 20/80 wt.%.

are clearly better than those of the PAN matrix. When the content of PC exceeds 70 wt.%, the gel-type polymer (PAN) loses its mechanical strength. However, the AG2 copolymer retains good mechanical strength. At a higher PC content (>90 wt.%), the composite of the copolymer and the PC can also form a film. The Young's modulus and toughness both increase with the content of the GMA-IDA unit. Notably, the GMA-IDA unit with a large polar side-chain can significantly improve the mechanical properties of the gel-type polymer electrolytes.

3.2. Environment of lithium ion doped in gel-type polymer electrolytes

Scheme 2 indicates the possible coordination sites of lithium ions, including the carbonyl groups of GMA-IDA, the N atoms of the chelating groups, the C≡N groups, and PC.

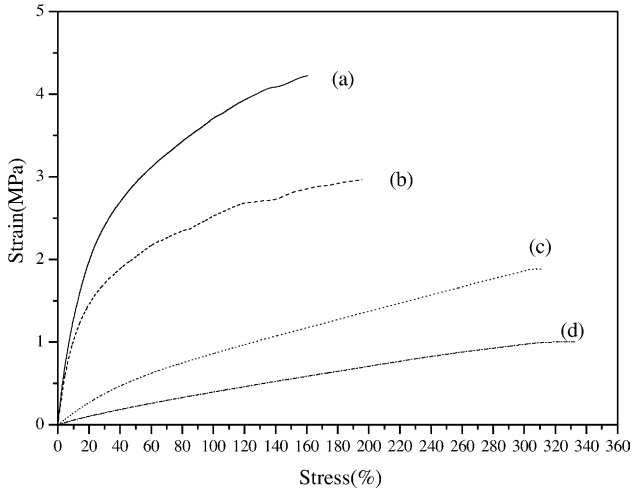

Fig. 4. Stress–strain test for AG2 with various PC content: (a) AG2/PC = 50/50 wt.%, (b) AG2/PC = 40/60 wt.%, (c) AG2/PC = 30/70 wt.%, and (d) AG2/PC = 20/80 wt.%.

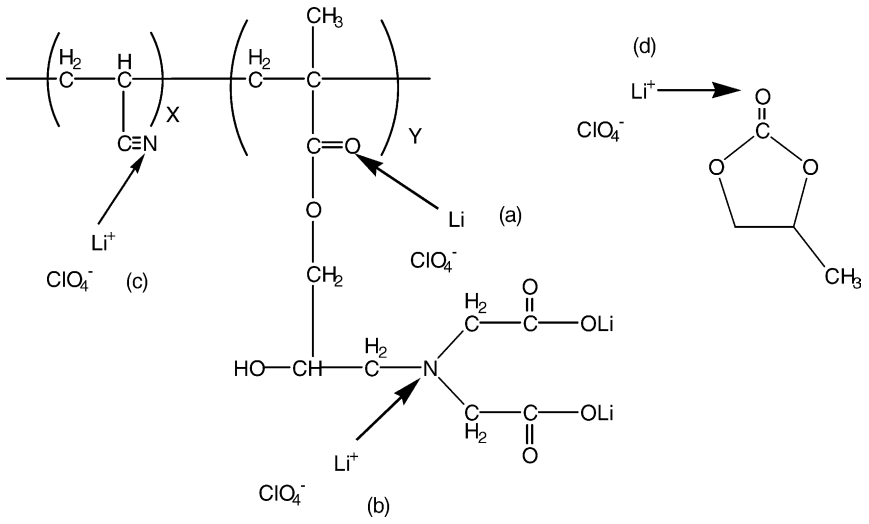

Scheme 2. Schematic representation of coordination of lithium ions to different positions: (a) to the carbonyl oxygens, (b) to the nitrogen atoms of chelated groups, (c) to the CN groups, (d) to the plasticizer (PC).

FT-IR was employed to investigate the interaction between functional groups with different amount of lithium salt doped into the gel-type copolymer.

Fig. 5 shows the IR spectra of the ring bending mode of PC (at 715 cm^{-1}) for various $LiClO_4$ contents. A shoulder appeared in the high frequency region (722 cm^{-1}) as the content of the $LiClO_4$ increased, because of the interaction between lithium ion and PC, which mainly occurred on the carbonyl groups of the PC [20,27–30].

Fig. 6 displays the characteristics of FT-IR spectra for the absorbance of C=O on the PC molecules (1790 cm^{-1}) and the C=O bond of ester group (1730 cm^{-1}) under various concentrations of $LiClO_4$. A frequency of the band that corresponds to the C=O stretching vibration of PC downward as the amount of $LiClO_4$ is increased, which is attributable to interactions between lithium ions and the C=O group of PC [30]. In contrast, no such change is exhibited in the stretching region of the C=O band of ester group [19,20,38]. In this system, the interactions between the lithium ion and ester group is relatively weak or not exist. The lithium ions prefer to coordinate with other groups [25,31]. Therefore, no significant effect on the ester group is observed.

Moreover, IR spectra analysis was used to elucidate the possible interaction between the C≡N group of the copolymer and the lithium ions. Fig. 7 shows the evolution of the C≡N stretching band in the IR spectra of AG2/PC = 50/50 wt.% for various concentrations of $LiClO_4$. A small but obvious variation at the high frequency side (2270 cm^{-1}) associated

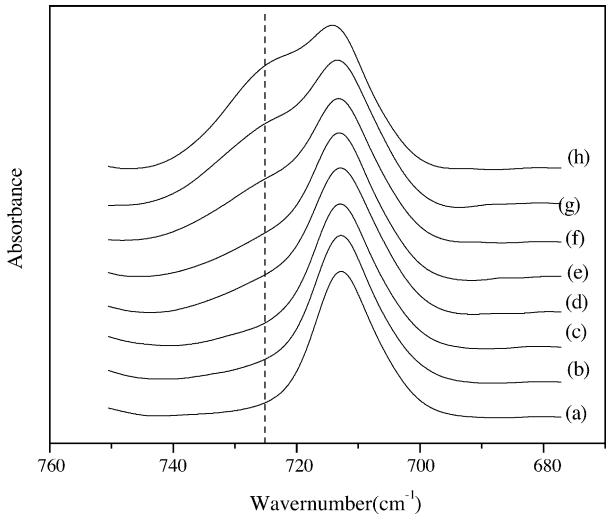

Fig. 5. FT-IR spectra for the symmetric ring deformation of PC in AG2/PC = 50/50 wt.% with various $LiClO_4$ concentrations: (a) 0.0 mmol (g-polymer)$^{-1}$, (b) 0.25 mmol (g-polymer)$^{-1}$, (c) 0.5 mmol (g-polymer)$^{-1}$, (d) 1.0 mmol (g-polymer)$^{-1}$, (e) 1.5 mmol (g-polymer)$^{-1}$, (f) 2.0 mmol (g-polymer)$^{-1}$, (g) 3.0 mmol (g-polymer)$^{-1}$, (h) 4.0 mmol (g-polymer)$^{-1}$.

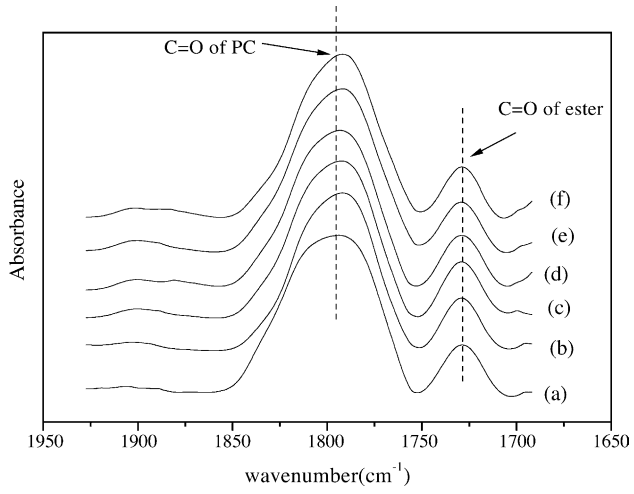

Fig. 6. FT-IR spectra for the –C=O groups of PC and ester in AG2/PC = 50/50 wt.% with various $LiClO_4$ concentrations: (a) 0.0 mmol (g-polymer)$^{-1}$, (b) 0.25 mmol (g-polymer)$^{-1}$, (c) 0.5 mmol (g-polymer)$^{-1}$, (d) 1.0 mmol (g-polymer)$^{-1}$, (e) 1.5 mmol (g-polymer)$^{-1}$, (f) 2.0 mmol (g-polymer)$^{-1}$.

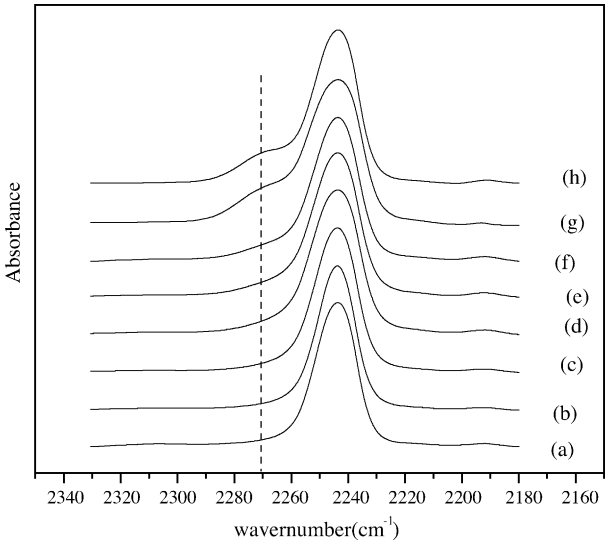

Fig. 7. FT-IR spectra for the CN group in AG2/PC = 50/50 wt.% with various $LiClO_4$ concentrations: (a) 0.0 mmol (g-polymer)$^{-1}$, (b) 0.25 mmol (g-polymer)$^{-1}$, (c) 0.5 mmol (g-polymer)$^{-1}$, (d) 1.0 mmol (g-polymer)$^{-1}$, (e) 1.5 mmol (g-polymer)$^{-1}$, (f) 2.0 mmol (g-polymer)$^{-1}$, (g) 3.0 mmol (g-polymer)$^{-1}$, (h) 4.0 mmol (g-polymer)$^{-1}$.

with the symmetric C≡N stretching mode, can be observed. The shoulder at around 2270 cm^{-1} is regarded as coming from he interaction between lithium ions and C≡N groups [27,28,32,38]. However, there are two factors causing that the shoulder is unobvious. First, the bonding of C≡N is very strong. Ordinary interactions cannot easily to influence the IR band of C≡N group [32]. It is more obvious, especially when the concentration of lithium ions is low. The other factor is that the lithium ions interact with other groups in the gel-type polymer electrolytes. As shown in FT-IR spectra, lithium ions could interact with PC, leading to restriction of the lithium ions coordinating with the C≡N groups [33]. Accordingly the stretch band of the C≡N group does not change clearly, even when the concentration of the lithium salt is increased to 2 mmol (g-polymer)$^{-1}$. In brief summary, this study has established that lithium ions interact with PC and the C≡N group of polymer. However, the spectrum of C–N band is overlaid by other peaks, so that it is difficult to distinguish.

Lithium ions in the gel-type polymer electrolytes influence the interaction of PC with the lithium ions of –COO^-Li^+ groups. The IR spectra for the –COO^- stretching region of iminodiacetic acid are also obtained, as shown in Figs. 8 and 9. Fig. 8 displays the IR spectra of gel-type polymer electrolytes with various concentrations of $LiClO_4$. As the concentration of $LiClO_4$ increases, a shoulder appears at the higher frequency (1675 cm^{-1}). Fig. 9 shows the IR spectra of gel-type polymer electrolytes with various PC contents. However, the intensity of the shoulder peak at 1675 cm^{-1} declines as PC content rises. This phenomenon can be described as lithium ions replace –COO^-Li^+ in interacting with the PC when the PC content is low, as revealed by Scheme 3. Additionally, as the PC content in the GPE increases, freer PC molecules that do not interact with

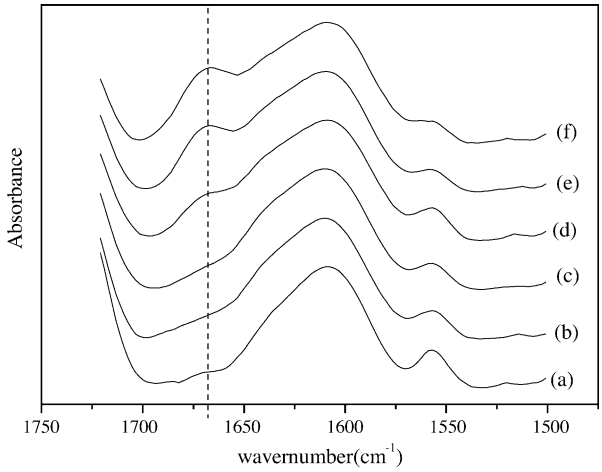

Fig. 8. FT-IR spectra for the –COO^- group in AG2/PC = 50/50 wt.% with various $LiClO_4$ concentrations: (a) 0.0 mmol (g-polymer), (b) 0.25 mmol (g-polymer), (c) 0.5 mmol (g-polymer), (d) 1.0 mmol (g-polymer), (e) 1.5 mmol (g-polymer), and (f) 2.0 mmol (g-polymer)$^{-1}$.

–COO^-Li^+ are generated. Therefore, when more lithium ions are added to GPE, the lithium ions preferentially coordinate with the freer PC molecules, reducing the intensity of the shoulder peak.

^{7}Li magic angle spinning (MAS) NMR spectra of gel-type polymer electrolytes with various $LiClO_4$ concentrations, corresponding to the chelating groups of GMA-IDA units, PC and C≡N groups, were obtained. Fig. 10 displays high-resolution ^{7}Li MAS NMR spectra and demonstrates the presence of four distinct lithium ion sites in the gel-type polymer electrolytes. Four peaks with well-resolved resonance are observed as the temperature is reduced. Spinning sidebands are also observed at low temperatures, establishing that the ^{7}Li quadrupolar interaction is increased by a decrease in the mobility of the lithium ions as the temperature is reduced. However, raising the temperature causes these four peaks to shift together, until they eventually combine into a sin-

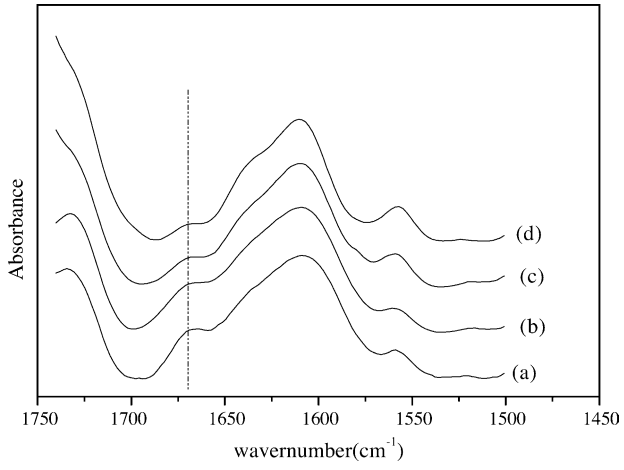

Fig. 9. FT-IR spectra for the –COO^- group with 2 mmol $LiClO_4$ (g-polymer)$^{-1}$ in: (a) AG2/PC = 50/50 wt.%, (b) AG2/PC = 40/60 wt.%, (c) AG2/PC = 30/70 wt.%, and (d) AG2/PC = 20/80 wt.%.

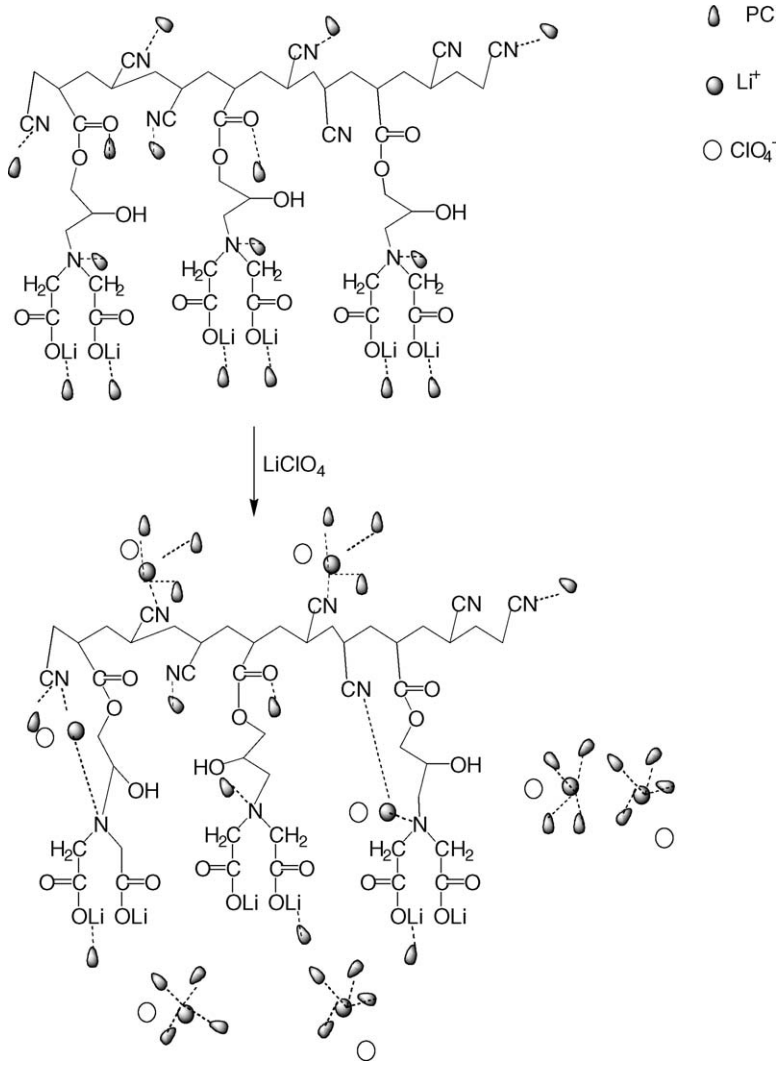

Scheme 3. Schematic representation of that the doping lithium ions effect the interaction of PC with $–COO^{-}Li^{+}$ groups.

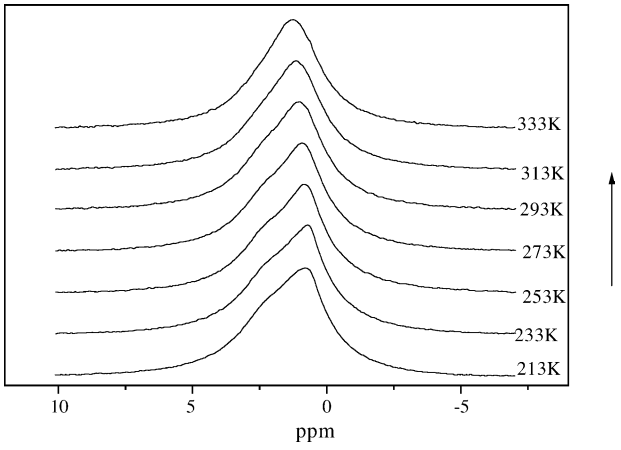

Fig. 10. Variable–temperature ^{7}Li proton-decoupled MAS NMR spectra of AG10/PC = 50/50 wt.% doped with 0.25 mmol $LiClO_4$ (g-polymer)$^{-1}$.

gle resonance. Classical peak merging involves a two-site exchanging process, and normally a temperature-dependent site preference [34,35]. According to Wen et al. [34], the frequency of the jumps among the four sites (Sites 1, 2, 3, 4) must be greater than the separation of the four resonance peaks, since the peaks are present at low temperature. Consequently, the frequency of separation must exceed 100 Hz, for Sites 1, 2, 3 and 4, so that the peaks coalesce as the mobility of the lithium ions increases. At temperatures over 263 K, the exchange process is fast, relative to the NMR time scale, resulting in a single resonance with a chemical shift that is the weight average of the individual components.

Fig. 11 shows the solid-state ^{7}Li NMR spectra for various lithium salt concentrations at 213 K. As discussed above, the four distinct resonance peaks are observed and well resolved when the amounts of doped lithium salt are high. After the deconvolution of AG10/PC = 50/50 wt.% without the lithium salt in Fig. 11(a), Site 1, Site 2 and Site 3 are observed and their linewidth is compared, as described elsewhere

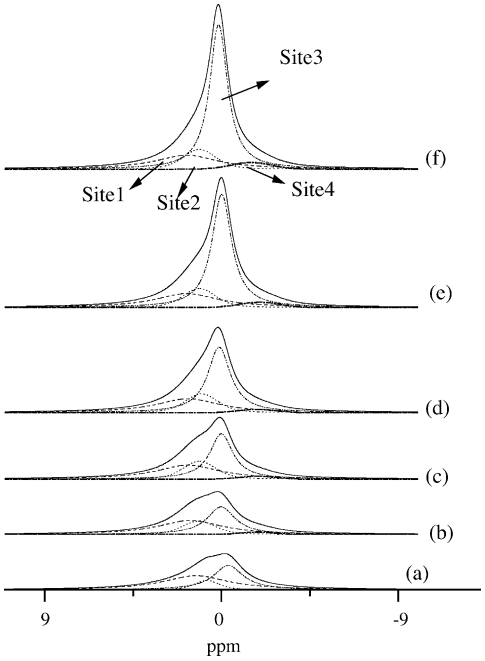

Fig. 11. Deconvolution of ^{7}Li proton-decoupled MAS NMR spectra at 213 K for AG10/PC = 50/50 wt.% doped with: (a) 0.0 mmol $LiClO_4$ (g-polymer)$^{-1}$, (b) 0.25 mmol $LiClO_4$ (g-polymer)$^{-1}$, (c) 0.5 mmol $LiClO_4$ (g-polymer)$^{-1}$, (d) 1.0 mmol $LiClO_4$ (g-polymer)$^{-1}$, (e) 1.5 mmol $LiClO_4$ (g-polymer)$^{-1}$, and (f) 2.0 mmol $LiClO_4$ (g-polymer)$^{-1}$.

[25,32,36]. Site 1 is associated with the –COO^-Li^+ groups in the GMA-IDA unit. Site 2 is attributed to the coordination between the nitrogen atoms on the GMA-IDA units and the lithium ions, which are dissociated from the –COO^-Li^+ group of the GMA-IDA. Site 3 is related to the coordination between the PC and the lithium ions, which are derived from the copolymer. The increase in intensity associated with Site 2 and Site 3 follows from the interaction between the groups and the doped lithium salt. Notably, as the doping concentration of lithium salt is increased to 0.25 mmol $LiClO_4$ (g-polymer)$^{-1}$, Site 4 appears, and the intensity associated with Site 2 markedly exceeds that associated with Site 3 in Fig. 11, indicating that the lithium ion is preferentially coordinated to Site 2. Additionally, the intensities of Sites 2, 3 and 4 raise with the lithium salt content, as shown in Fig. 11. The chelating group interacts with the lithium ions more strongly than do those of PC and the C≡N group because the unpaired electron on the nitrogen atom has a higher donicity. Moreover, Site 4 is only observed after the doping with lithium salt and the intensities of Site 2, Site 3 and Site 4 depended on the salt concentration. The linewidth of an NMR peak is well known to reflect the ion mobility in the system. More quickly moving ions yield a narrower peak. The narrower peak associated with Site 3 is caused by the fast-moving ions within PC. The broad Site 2 and Site 4 correspond to the slowing ions coordinated with the nitrogen atoms on the chelating groups and the C≡N groups of the polymer matrix, and the widest peak associated with Site1 correlated with the slowest-moving ions of the –COO^-Li^+ groups. The plasticizer is the main element

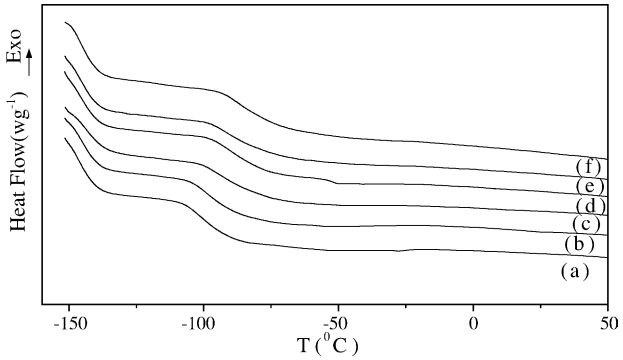

Fig. 12. DSC thermograms for AG2/PC = 40/60 wt.% doped with various $LiClO_4$ concentrations: (a) 0.0 mmol (g-polymer)$^{-1}$, (b) 0.25 mmol (g-polymer)$^{-1}$, (c) 0.5 mmol (g-polymer)$^{-1}$, (d) 1.0 mmol (g-polymer)$^{-1}$, (e) 1.5 mmol (g-polymer)$^{-1}$, and (f) 2.0 mmol (g-polymer)$^{-1}$.

in the gel-type electrolytes, so fast ion transport within plasticizer is the major contributor to the high conductivity of the gel-type polymer electrolytes.

In conclusion, FT-IR and solid-state ^{7}Li NMR spectra are effective methods for probing the different local environments of lithium ions in a GPE. The interactions of lithium ions with the PC and the groups in the copolymer, which contains the unpaired electron, are evidenced by the DSC studies, described below.

3.3. Thermal characteristics

DSC was employed to elucidate the effect of $LiClO_4$ and the plasticizer on the thermal behavior. The system of PAN-based GPEs has been determined by X-ray diffraction to be free of crystallinity [11]. Fig. 12 displays the DSC thermogram of samples (AG2/PC = 40/60 wt. %) with various concentrations of $LiClO_4$. A strong glass transition step at lower temperature is observed. Fig. 13 presents glass

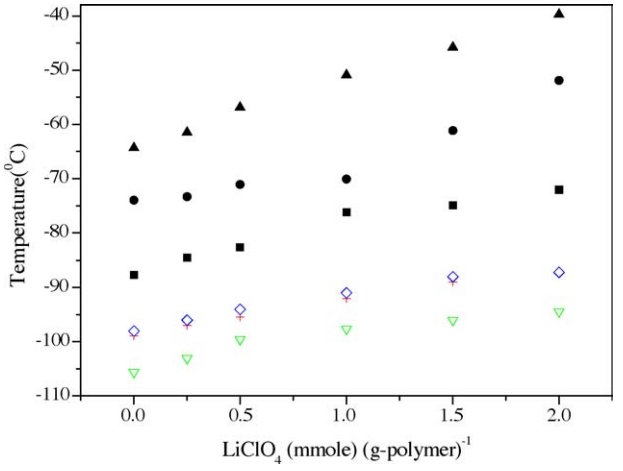

Fig. 13. The T_g vs. $LiClO_4$ concentration for (▲) AG10/PC = 50/50 wt.%, (●) AG6/PC = 50/50 wt.%, (■) AG2/PC = 50/50 wt.%, (◊) AG10/PC = 20/80 wt.%, (+) AG6/PC = 20/80 wt %, and (▽) AG2/PC = 20/80 wt.%.

transition temperatures for the different compositions investigated herein. Different contents of plasticizer are mixed with the copolymers to determine the effects of plasticizer on thermal behavior. As expected, T_g decreases as the plasticizer concentration increase, because the PC molecules increase the distance between the polymer chains and so increase the movement of the PC molecules. However, the value of T_g increases with the concentration of lithium salt. These phenomena are similar to those exhibited by polyether-based polymer electrolytes, which are attributed to the effective cross-linking of polyether segments by the cations. The elevation of T_g in the gel-type polymer electrolytes is attributable to the polymer–lithium ion–PC interaction, and that between single lithium ions and PC. The interactions were confirmed by FT-IR analysis. Increasing the amount of lithium salt promotes the occurrence of interactions, reducing the motion of PC. Thus, T_g increases with the salt concentration.

3.4. Ionic conductivity

The ionic conductivity of the gel-type polymer electrolytes was measured using two stainless steel electrodes plates at different temperatures to study the conduction behavior of the charge carriers in the plasticized copolymers. The effect of copolymer composition on the ionic conductivity was initially investigated at different temperatures and with various plasticizer contents. Fig. 14 plots the variation in the ionic conductivity with copolymer composition at two plasticizer contents at 30 °C. At the lower PC content, the conductivity substantially declines as the number of GMA-IDA units in the copolymer increases, as shown in Fig. 14(a). At a higher PC content, the AG2 system has the highest conductivity of all the GPEs in this research, as shown in Fig. 14(b). This result maybe attributed to the strong interaction between PC and the $–COO^-Li^+$ group. According to the above results of FT-IR, the interactions between PC and $–COO^-Li^+$ groups can improve the mobility of lithium ions in the $–COO^-Li^+$ groups. The mobility of the lithium ions in the $–COO^-Li^+$ group increases with the PC content, so the charge carries from $–COO^-Li^+$, improving the ionic conductivity. Additionally, GMA-IDA unit restricts the molecular movements of PC. Therefore, T_g increases with the number of GMA-IDA units, and reduces the ionic mobility. Consequently, these two opposing effects determine the maximum ionic conductivity, as shown in Fig. 14(b). However, AG2/PC = 20/80 wt.% doped with 2 mmol $LiClO_4$ (g-polymer)$^{-1}$ has the highest conductivity, 2.17×10^{-3} S cm^{-1}, at 30 °C. This conductivity is higher than that of the typical GPEs, 1.70×10^{-3} S cm^{-1}, based on the PAN system with the same composition.

Fig. 14 plots the conductivity of polymer/PC = 50/50 wt.% as a function of lithium salt content at 30 °C. The conductivity increases with the salt concentration, and that of the PAN-based system reaches a maximum when the concentration of $LiClO_4$ is 1.5 mmol (g-polymer)$^{-1}$. However, it declines beyond this value. The phenomenon is similar to that reported

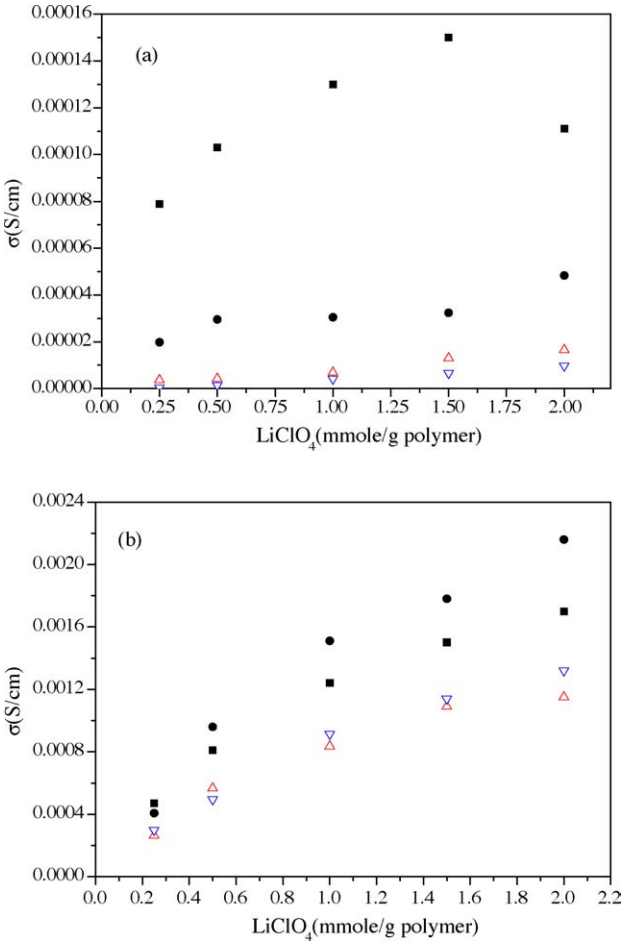

Fig. 14. (a) Ionic conductivity vs. $LiClO_4$ concentration for: (△) AG10/PC = 50/50 wt.%; (▽) AG6/PC = 50/50 wt.%; (●) AG2/PC = 50/50 wt.%; (■) PAN/PC = 50/50 wt.%. (b) Ionic conductivity vs. $LiClO_4$ concentration for: (△) AG10/PC = 20/80 wt.%; (▽) AG6/PC = 20/80 wt.%; (●) AG2/PC = 20/80 wt.%; (■) PAN/PC = 20/80 wt.%.

in the literatures [13,25,39–45]. At low concentrations of $LiClO_4$, the lithium salt is completely dissociated, and the number of mobile ions increases with the lithium salt concentration. At higher concentrations of $LiClO_4$, the dissociated ions of Li^+ and ClO_4^- could form ion-pairs. Fortunately, the GMA-IDA unit with the chelating group promotes the dissociation of Li^+ and ClO_4^- at higher $LiClO_4$ concentrations because the GMA-IDA units strongly interact with Li^+. Therefore, the existence of GMA-IDA units in the copolymer helps the lithium salt dissociate completely at higher $LiClO_4$ concentrations, increasing the number of charge carriers. These interactions between the GMA-IDA units and lithium ions are also evidenced by solid-state NMR spectra, as mentioned above.

The conductivity of PAN-based GPEs could be found elsewhere in the literatures [4,11,13,37]. Conductivity varies with temperature, according to either the Vogel–Tamman–Fulcher (VTF; Eq. (1)) relationship or the Arrhenius (Eq. (2)) relationship, depending on over which limited temperature range

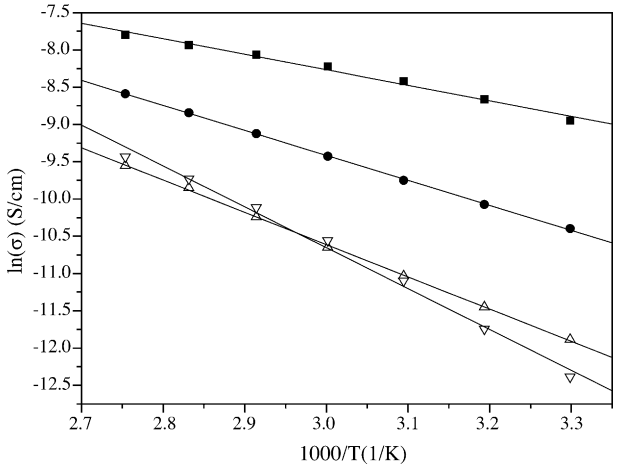

Fig. 15. Arrhenius plots of ionic conductivity for composite gel-type electrolytes doped with 1 mmol $LiClO_4$ (g-polymer)$^{-1}$: (△) AG10/PC = 50/50 wt.%; (▽) AG6/PC = 50/50 wt.%; (●) AG2/PC = 50/50 wt.%; (■) PAN/PC = 50/50 wt.%.

the conductivity was measured.

$$\sigma = AT^{-1/2} \exp[-B/k(T - T_0)] \quad (1)$$

$$\sigma = \sigma_0 \exp(-E_a/kT) \quad (2)$$

where A is a constant; E_a the activation energy; B the pseudo-activation energy related to segmental motion; k the Boltzmann constant; and T_0 the reference temperature that is normally related to T_g at which the free volume disappears, or the temperature at which the configurational entropy is zero. In most of the cases, T_0 is ca. 30–50 K below T_g of the polymer matrix.

Figs. 15 and 16 present the Arrhenius plots for PAN, AG2, AG6 and AG10 with a constant concentration of lithium salt, and PC 50 and 80 wt.%. All curves are straight lines at temperatures from 30 to 90 °C. All of the figures reveal that the

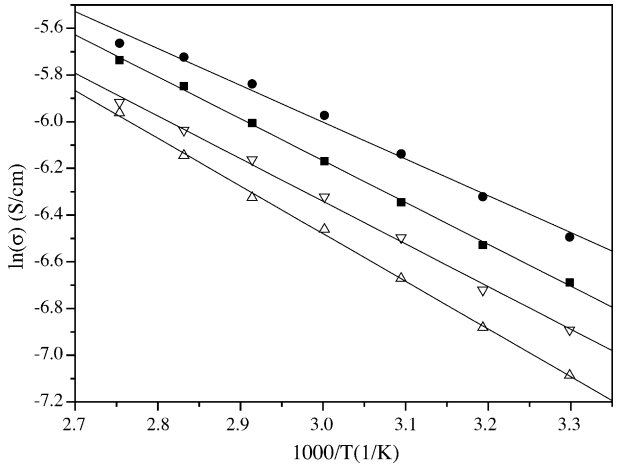

Fig. 16. Arrhenius plots of ionic conductivity for composite gel-type electrolytes doped with 1 mmol $LiClO_4$ (g-polymer)$^{-1}$: (△) AG10/PC = 20/80 wt.%; (▽) AG6/PC = 20/80 wt.%; (●) AG2/PC = 20/80 wt.%; (■) PAN/PC = 20/80 wt.%.

Table 4A
The activation energy range of conductivity for the gel-type polymer electrolytes calculated from Arrhenius equation

Composition	E_a (kJ mol^{-1})		
	AG2	AG6	AG10
Polymer/PC = 50/50 wt.%	20–32	35–40	45–54
Polymer/PC = 40/60 wt.%	15–20	21–26	20–27
Polymer/PC = 30/70 wt.%	14–16	16–21	16–21
Polymer/PC = 20/80 wt.%	11–15	14–19	12–19

Table 4B
The σ_0 of conductivity for AG2/PC = 20/80 wt.% with $LiClO_4$ (2 mmol (g-polymer)$^{-1}$) calculated from Arrhenius equation

Composition	ln(σ_0)		
	AG2	AG6	AG10
Polymer/PC = 50/50 wt.%	2.74	4.47	7.28
Polymer/PC = 40/60 wt.%	−0.77	0.33	0.80
Polymer/PC = 30/70 wt.%	−1.19	0.09	0.68
Polymer/PC = 20/80 wt.%	−1.45	−0.23	0.31

conductivity of the composites investigated herein followed an Arrhenius relationship for ion transport, indicating that the conductive environment of lithium ions in the GPEs is liquid-like and remains unchanged in the measurement temperature region.

The activation energy (E_a) of the conductivity for the gel-type polymer electrolytes was also calculated from Arrhenius equation. Table 4A summarizes all related values. The activation energy increases with the number of GMA-IDA units. The above discussion of DSC shows that the movement of PC decreases as the GMA-IDA content increases, increasing the activation energy. The σ_0 is a constant proportional to the number of carrier ions; Table 4B summarizes all related values. The carrier number increases with the GMA-IDA unit, due to the –COO^- Li^+ group in the GMA-IDA unit will increase the Li^+ ion. With the same copolymer, the σ_0 decreases with the increasing of the PC plasticizer content. As the content of the PC plasticizer increases, the concentration of lithium ion decreases in the system, therefore, the σ_0 decreases in the system.

4. Conclusion

Gel-type polymer electrolyte was synthesized from AN and GMA-IDA complexes with $LiClO_4$ and PC. The results reveal a significant interaction between the lithium ions and PC, the C≡N groups and the chelating groups on the GMA-IDA units. ^{7}Li MAS NMR was used to characterize the local environment of the lithium ions and established that the order of the interaction of lithium ions was chelating group on the GMA-IDA > plasticizer > C≡N group. These interactions cause T_g to increase with the salt concentration and the GMA-IDA content. The maximum conductivity measured in this work exceeded that of the typical PAN-based system with same compositions. The results reveal that increasing the

number of chelating groups in the copolymer can increase the content of charge carriers, improving the conductivity of the gel-type polymer electrolyte. Incorporating GMA-IDA units in the copolymers also improves the mechanical characteristics.

Acknowledgements

The authors thank the Ministry of Economic Affairs of the Taiwan for financially support under Contract No. TDPA:91-EC-17-A-05-S1-0014. Assistance from Ms. S.Y. Sun of the NSC Instrument Center at NCKU in conducting solid-state NMR experiments was greatly appreciated.

References

[1] J.R. MacCallum, C.A. Vincent, Polymer Electrolytes Reviews, Elsevier, London, 1987.
[2] F.M. Gray, Solid Polymer Electrolytes, VCH Publishers, New York, 1991.
[3] D.E. Fenton, J.M. Parker, P.V. Wright, Polymer 14 (1973) 589.
[4] K.M. Abraham, M. Alamgir, J. Electrochem. Soc. 137 (1990) 1657.
[5] F. Croce, F. Gerace, G. Dautzemberg, S. Passerini, G.B. Appetecchi, B. Scrosati, Electrochim. Acta 39 (1994) 2187–2194.
[6] D. Peramunage, D.M. Pasluariello, K.M. Abraham, J. Electrochim. Soc. 142 (1995) 1789–1790.
[7] H.S. Choe, J. Giaccai, M. Alamgir, K.M. Abraham, Electrochim. Acta 40 (1995) 2289–2293.
[8] J.M. Tarascon, A.S. Gozdz, C.N. Schmutz, F. Shokoohi, P.C. Warren, Solid State Ion. 86–88 (1996) 49–54.
[9] G.B. Appetecchi, F. Croce, B. Scrosati, Electrochim Acta 40 (1995) 991–997.
[10] X. Lin, T. Osaka, J. Electrochem. Soc. 144 (1997) 3066–3071.
[11] M. Watanabe, M. Kanba, K. Nagaoka, I. Shinoara, J. Polym. Sci.: Polym. Phys. 21 (1983) 939–948.
[12] E. Cazzanelli, G. Matriotto, G.B. Appetecchi, F. Croce, B. Scrosati, Electrochim. Acta 40 (1995) 2379–2382.
[13] B. Huang, Z. Wang, G. Li, H. Huang, R. Xue, L. Chen, F. Wang, Solid State Ion. 85 (1996) 79–84.
[14] H. Huang, L. Chen, X. Hung, R. Xue, Electrochim. Acta 37 (1992) 1671–1673.
[15] S. Hyodo, K. Okabayashi, Electrochim. Acta 34 (1989) 1551–1556.
[16] D. Battisti, G.A. Nazri, B. Klassen, R. Aroca, J. Phys. Chem. 97 (1933) 5826–5830.
[17] D. Ostrovskii, L.M. Torell, G.B. Appetecchi, B. Scrosati, Solid State Ion. 106 (1998) 19–24.
[18] D. Ostrovskii, A. Brodin, L.M. Torell, J. Chem. Phys. 109 (1998) 7618–7624.
[19] C.S. Kim, S.M. Oh, Electrochim. Acta 45 (2000) 2101–2109.
[20] P. Johansson, M. Edvardsson, J. Adebahr, P. Jacobsson, J. Phys. Chem. B 107 (2003) 12622–12627.
[21] D. Ostrovskii, P. Johansson, J. Electrochem. Soc. 149 (2002) A662–A666.
[22] C.C. Wang, C.C. Chang, C.Y. Chen, Macromol. Chem. Phys. 202 (2001) 882–890.
[23] C.C. Wang, C.Y. Chen, J. Appl. Polym. Sci. 85 (2002) 919–928.
[24] C.C. Wang, C.Y. Chen, C.C. Chang, J. Appl. Polym. Sci. 84 (2002) 1353–1362.
[25] W.H. Hou, C.C. Wang, C.Y. Chen, Polymer 44 (2003) 2983–2991.
[26] C.Y. Chen, C.Y. Chen, J. Appl. Polym. Sci. 86 (2002) 1986–1994.
[27] Z. Wang, B. Huang, Z. Lu, S. Wang, R. Xue, L. Chen, F. Wang, Spectrochim. Acta Part A 52 (1996) 691–703.
[28] Z. Wang, B. Huang, S. Wang, R. Xue, L. Chen, J. Electrochem. Soc. 144 (1997) 778–786.
[29] S.R. Starkey, R. Frech, Electrochimica. Acta 42 (1997) 471–474.
[30] D. Battisti, G.A. Nazri, B. Klassen, R. Aroca, J. Phys. Chem. 97 (1993) 5826–5830.
[31] E. Cazzanell, G. Mariotto, G.B. Appetecch, F. Corce, B. Scrosati, Electrochem. Acta 40 (1995) 2379–2382.
[32] Z. Wang, B. Huang, R. Xue, X. Huang, L. Chen, Solid State Ion. 121 (1999) 141–156.
[33] T.C. Wen, H.H. Kuo, A. Gopalan, Macromolecules 34 (2001) 2958–2963.
[34] H.L. Wang, H.H. Kuo, T.C. Wen, Macromolecules 33 (2000) 6910–6912.
[35] A. Abragam, The Principle of Nuclear Magnetism, Oxford University Press, Oxford, 1961.
[36] B. Huang, Z. Wang, L. Chen, R. Xue, F. Wang, Solid State Ion. 91 (1996) 279–284.
[37] F. Croce, S.D. Broen, S.G. Greenbaum, S.M. Slane, M. Salomon, Chem. Mater. 5 (1993) 1268–1272.
[38] Z. Florjanczyk, E. Zygadlo-Monikowska, W. Wieczorek, A. Ryszawy, A. Tomaszewska, K. Fredman, D. Golodnitsky, E. Peled, B. Scrosati, J. Phys. Chem. B 108 (2004) 14907–14914.
[39] S.M. Lee, W.L. Yeh, C.C. Wang, C.Y. Chen, Electrochim. Acta 49 (2004) 2667–2673.
[40] W.H. Hou, C.C. Wang, C.Y. Chen, Solid State Ion. 166 (2004) 397–405.
[41] S.M. Lee, C.C. Wang, C.Y. Chen, Electrochim. Acta 48 (2003) 3699–3708.
[42] W.H. Hou, C.C. Wang, C.Y. Chen, Electrochim. Acta 48 (2003) 679–690.
[43] S.M. Lee, C.C. Wang, C.Y. Chen, Electrochim. Acta 48 (2003) 669–677.
[44] S.M. Lee, C.C. Wang, C.Y. Chen, Electrochim. Acta 49 (2004) 4907–4913.
[45] W.H. Hou, C.C. Wang, C.Y. Chen, Electrochim. Acta 49 (2004) 2105–2112.